In-Situ Studies of the Electrochemical Reduction of Supported Ultrathin Single Crystalline RuO_2(110) Layer in Acidic Environment

*Tim Weber[a,b], Marcel J. S. Abb[a,b], Omeir Khalid[a,b], Johannes Pfrommer[c,d], Francesco Carla[e], Raja Znaiguia[e], Vedran Vonk[c,d], Andreas Stierle[c,d], Herbert Over[a,b]**

a) *Physikalisch-Chemisches Institut, Justus Liebig University, Heinrich-Buff-Ring 17, 35392 Giessen, Germany*
b) *Zentrum für Materialforschung, Justus Liebig University, Heinrich-Buff-Ring 16, 35392 Giessen, Germany*
c) *Deutsches Elektronen-Synchrotron (DESY), D-22607 Hamburg, Germany*
d) *Fachbereich Physik University Hamburg, Jungiusstrasse 9, D-20355 Hamburg, Germany*
e) *ID03 – Surface Diffraction Beamline, European Synchrotron Radiation Facility (ESRF), 71 Avenue des Martyrs, 38000 Grenoble, France*

* *Corresponding authors:* E-mail: Herbert.Over@phys.chemie.uni-giessen.de

Abstract

With *in-situ* surface X-ray diffraction (SXRD) and X-ray reflectivity (XRR) in combination with ex-situ characterization by scanning electron microscopy (SEM), X-ray photoelectron spectroscopy (XPS), and cyclic voltammetry (CV) the electrochemical reduction of an ultrathin (1.66 nm thick) single crystalline RuO_2(110) layer supported of Ru(0001) was studied in acidic environment, providing clear-cut evidence and mechanistic details for the transformation of RuO_2 towards hydrous RuO_2 and metallic Ru. The reduction process proceeds via proton insertion into the RuO_2(110) lattice. For electrode potentials (0 to -50mV vs. SHE) the layer spacing of RuO_2(110) increased, maintaining the octahedral coordination of Ru (SXRD). Continuing proton insertion at -100 to -150 mV leads to transformation of lattice oxygen of RuO_2 to OH and water that destroys the connectivity among the Ru octahedrons and eventually to the loss of crystallinity (SXRD) in the RuO_2(110) film at -200 mV accompanied by a swelling of the layer with well-defined thickness (XRR). During the protonation process soluble Ru-complexes may form. XPS provide evidence for the transformation of RuO_2(110) to a hydrous RuO_2 layer, a process that proceeds first homogenously and at higher cathodic potentials heterogeneously by re-deposition of a previously dissolved Ru complexes.

1. Introduction

Electrochemical water splitting (electrolysis) will be important for a sustainable hydrogen economy[1] in that intermittent wind and solar energy resources can be stored in chemical bonds, such as in H_2, and can either be used directly to power vehicles and stationary devices or can readily be transformed back to electric energy by proton-exchange membrane (PEM) fuel cells whenever there is demand.[2] The electrochemical hydrogen evolution reaction (HER) takes place at the cathode of water electrolysers.[3] The HER has even been considered a prototype reaction in surface electrochemistry[4-6], since the reaction comprises a two-electron transfer[7] and is therefore much simpler than for instance the four-electron process of the oxygen evolution reaction (OER), the anodic reaction of a water electrolyser.

Various metals have been identified to be active HER electrocatalysts in acidic media, most notably platinum and various Pt alloys[8,9], while oxides are in general considered to be inferior in the HER. This simplified view is not reconciled with RuO_2 and IrO_2.[10-17] RuO_2 is actually a remarkably efficient electrocatalyst for HER[10] that resists poisoning by heavy metals. Its activity in acid media is only slightly lower than that of platinum: the overpotential of RuO_2 is 50 mV higher at a current density of 0.1 A/cm^2 than that of Pt.[12] Accordingly, RuO_2-coated cathodes have also been investigated and applied in industry.[16,18] Even RuO_2-based anodes in the form of dimensionally stable anodes (DSA) can face HER conditions during the shutdown of a chlorine electrolyser, when it intermittently functions as a fuel cell and therefore the RuO_2 based coating as the cathode.[19]

However, reducible oxides are expected to be chemically unstable and are readily reduced to the corresponding metals in the HER potential region.[20] Indeed a hydroxylation process was reported for RuO_2/Ni cathodes under strongly alkaline HER conditions (10 M NaOH).[21,22] More recently, Näslund et al.[23] concluded from detailed XPS and XRD experiments of RuO_2 coatings deposited on Ni that RuO_2 is transformed to ruthenium oxyhydroxide phase, $RuO(OH)_2$, that further reduces to metallic ruthenium upon extended treatments in the HER potential region under strongly alkaline conditions (8 M NaOH). The Ru3d assignment of Näslund et al. was, however, challenged by Karlsson et al.[24] on the basis of density functional theory (DFT) calculated XPS shifts of Ru3d. The structure of the water-RuO_2(110) interface in 0.1 M NaOH solution was recently studied by *in-situ* surface X-ray diffraction (SXRD).[25] At a cathodic potential of -200 mV bridging OH and on-top water are formed in a low-density water layer.

However, for the electrochemical reduction of RuO_2 under acidic conditions *conflicting* results are reported in the literature. On RuO_2 thin film electrodes both x-ray diffraction (XRD)[26] and X-ray photoelectron spectroscopy (XPS)[27] show that neither the bulk nor the

surface region of the oxide is chemically reduced to hydrous RuO_2 or metallic ruthenium during the HER in 0.5 M H_2SO_4. XRD experiments indicate, however, a significant shift of the characteristic diffraction peaks of the RuO_2 thin film electrode to lower momentum transfers Q during cathodic polarization in the potential region of the HER.[28] The observed expansion of the unit cell of RuO_2 is ascribed to proton incorporation in the RuO_2 lattice and is found to be fully reversible as the characteristic diffraction peaks of RuO_2 move back to their original positions when the polarization is turned off. The shape of the Ru3d core level peaks of RuO_2 in ex-situ XPS does not change during cathodic treatment in the HER potential region. Therefore, Rochefort et al.[27] suggested that the atomic arrangement around each Ru center and the conformation of the RuO_6 octahedrons are not disturbed by H insertion into the oxide structure. Kötz and Stucki[12] concluded on the basis of ex-situ XPS studies that during cathodic treatment in the HER potential region under acidic conditions (0.5 M H_2SO_4) the surface of the polycrystalline RuO_2 electrode is only partly reduced to some oxy-hydroxide, but complete reduction to metallic Ru was excluded.

In two papers Lister et al.[29,30] studied with cyclic voltammetry (CV) and in-situ SXRD the electro-reduction of two orientations of single crystalline RuO_2, i.e., (110) and (100) in 0.5 M H_2SO_4. The CVs of RuO_2(100) and RuO_2(110) exhibit a reduction signature near the HER potential, indicating Ru-metal like behavior. SXRD reveals an expansion of the top RuO_2 layer, but no roughening of the surface and no Ru metal formation.

It is the main objective of the present paper to resolve these apparent discrepancies in the literature concerning the electrochemical reduction of RuO_2 in acidic environment by devising a model experiment. Here, we focus on the electrochemical stability of a 1.66 nm thick covering single-crystalline RuO_2(110) layer coated on Ru(0001) in the potential region of HER in acidic media (HCl, pH = 0.3), employing the *in-situ* techniques of surface X-ray diffraction (SXRD) and X-ray reflectivity (XRR) together with ex-situ characterization by scanning electron microscopy (SEM), X-ray photoelectron spectroscopy (XPS), and cyclic voltammetry (CV). This dedicated model electrode design allows one to follow structural and morphological changes of the RuO_2(110) film even in short time periods, thus being fully compatible with the imposed time constraints during typical synchrotron-radiation based experiments. With SXRD the crystallinity of the RuO_2(110), while with XRR the layer thickness and its roughness can be followed *in-situ* when varying the electrode potential to more cathodic potentials. The RuO_2(110) film turned out to be partially stable down to -150 mV with respect to standard hydrogen electrode (SHE), but at -200 mV vs SHE the crystallinity of RuO_2 was completely lost, while the layer structure was still maintained with increased thickness. On the basis of

post-XPS and CV experiments the chemical nature of the resulting electrochemically reduced RuO_2 film is identified with a hydrous RuO_2 layer and metallic ruthenium.

2. Experimental Section

The ultrathin RuO_2(110) film was grown epitaxially on a single crystalline hat-shaped Ru(0001) disk (7 mm diameter, MaTecK, Jülich, Germany) under ultrahigh vacuum (UHV) conditions. First, the Ru(0001) single crystal was sputtered with Ar^+ ions at the temperature of 380 °C for 20 minutes in order to clean the sample. Subsequently, the sample was heated up to 780 °C to smoothen the rough surface. Next, the sample was annealed at 780 °C for 20 min in an oxygen gas atmosphere of $p(O_2) = 2 \cdot 10^{-7}$ mbar to deplete the surface near region from carbon contamination. This two-step procedure was repeated several times until the low energy electron diffraction (LEED) pattern showed an intense hexagonal diffraction pattern (with low background) corresponding to a clean Ru(0001) surface. RuO_2(110) was grown on this Ru(0001) surface at a temperature of 380 °C with an oxygen pressure of $3 \cdot 10^{-5}$ mbar for 120 min.[31,32]

The *in-situ* surface X-ray diffraction (SXRD) and X-ray reflectivity (XRR) experiments were conducted at beamline ID03 at ESRF, Grenoble[33] equipped with a specifically constructed *in-situ* electrochemical (EC) flow cell.[33,34] The RuO_2(110)/Ru(0001) model electrode is housed in a special cavity at the bottom of the inner cylindrical hole, and the counter electrode consists of a glassy carbon rod at the top of the cell, with a similar electrode surface of 0.5 cm^2 as the working electrode. An Ag/AgCl electrode (3.4 M KCl) used as the reference electrode is located between the working and the glassy carbon counter electrode (CE). The electrode potential values are given *versus* the standard hydrogen electrode (SHE) throughout this paper. We used as electrolyte solution an aqueous 0.5 M HCl solution (pH = 0.3) prepared from HCl Suprapur® (Merck, Darmstadt, Germany) and high-purity water (18.2 MΩ·cm). HCl was chosen as electrolyte in order to reduce the overpotentials at the CE that oxidizes preferentially Cl^- rather than water (oxygen evolution reaction). The produced H_2 and Cl_2 are removed from the EC flow cell by exchanging the electrolyte solution. The employed potentiostat was a PAR VersaStat II (Princeton Applied Research).

First a full set of SXRD and XRR data were taken at open-circuit potential (OCP) in both water (OCP = 690 mV) and HCl (OCP = 150 mV). Subsequently we reduced the electrode potential of RuO_2(110) to 0 mV, -50 mV, -100 mV, -150 mV, or -200 mV by means of potentiostatic pulses with a duration of 30 s. During the first 10 s of a pulse no electrolyte flow was applied to the cell, whereas for the last 20 s the cell was purged with fresh electrolyte.

After each pulse the RuO_2(110)/Ru(0001) model electrode was set to a resting potential of 0 mV and purged with fresh electrolyte for another 10 s. The SXRD and XRR data were taken in between the pulses at the above mentioned resting potential; the data acquisition time was about 55 min. With this experimental protocol (potential pulse and going back to a rest potential of 0 mV between consecutive pulses) only irreversible changes of the RuO_2(110) layer can be studied. We checked for potential beam damages by measuring h- and l-scans before and after XRR experiments. No changes in the scans were observed.

The above described *in-situ* experiments were complemented by *ex-situ* characterization of the cathodically treated RuO_2(110) ultrathin films, including X-ray photoemission spectroscopy (XPS) experiments (PHI VersaProbe II), scanning electron microscopy (SEM) experiments (Zeiss Merlin) and cyclic voltammetry. XPS experiments were performed with the photon energy at 1486.6 eV (monochromatized Al-K_α line, excitation power ~40-50 W) and the X-ray spot size of ~200 µm. The pass energy was chosen to be 11.75 eV and the resolution was 0.5 eV (as determined with silver). The binding energy scale was calibrated with copper, gold and silver, so that for a conducting sample such as RuO_2(110)/Ru(0001) no further calibration is necessary. The SEM experiments were conducted with an acceleration voltage of 2 kV and a probe current of 100 pA. The micrographs were obtained with the secondary electron (SE2) detector.

Cyclic voltammetry was utilized to monitor possible alterations in the electrochemical response of the RuO_2(110) surface as a result of cathodic treatment. Accordingly, the protocol of the electrode potential variation used during the *in-situ* experiments was adapted: potentiostatic pulses (30 s) of the desired electrode potential were applied followed by setting the RuO_2(110) electrode to a resting potential of 0 mV for 55 min (time for acquiring the SXRD and XRR data at ID03). Subsequently, a cyclic voltammogram was recorded and the next potentiostatic pulse was applied. These experiments were conducted in an electrochemical glass cell utilizing an home-built electrode holder, so that only the oxidized surface of the Ru(0001) single crystal was exposed to the 0.5 M HCl solution. An Ag/AgCl electrode was used as RE, the CE consisted of a glassy carbon rod. The applied potentiostat was a SP-150 (BioLogic Science Instruments).

3. Results

For the SXRD experiments, l- and h-scans are defined by Ru(0001) sample (a = b = 2.71 Å, α = 120°, c = 4.28 Å, γ = 90°) with h and l oriented along the corresponding *a* and c directions in

reciprocal space (reciprocal direction k corresponds to an in-plane direction perpendicular to *a*). Further details can be found in previous report on the growth of RuO_2(110) on Ru(0001).[35] In **Figure 1** we summarize the SXRD data in the form of l- and h-scans depending on the applied electrode potential. The h-scans monitor the lateral periodicity, while the l-scans provide information on the layer spacing and the thickness of the layer. At open-circuit potential (OCP), the h-scan for l = 1.3 and k = 0 indicates clear peaks at h = 0.733 and h = 1.47, that are characteristic for a single crystalline RuO_2(110) film grown on Ru(0001) with high degree of lateral order.[35] The peak at h = 1 belongs to the first-order crystal truncation rod of Ru(0001) that is quite sensitive to the roughness of the RuO_2(110)/Ru(0001) interface. Other diffraction peaks are not discernible in the h-scan ranging from 0.3 to 1.6.

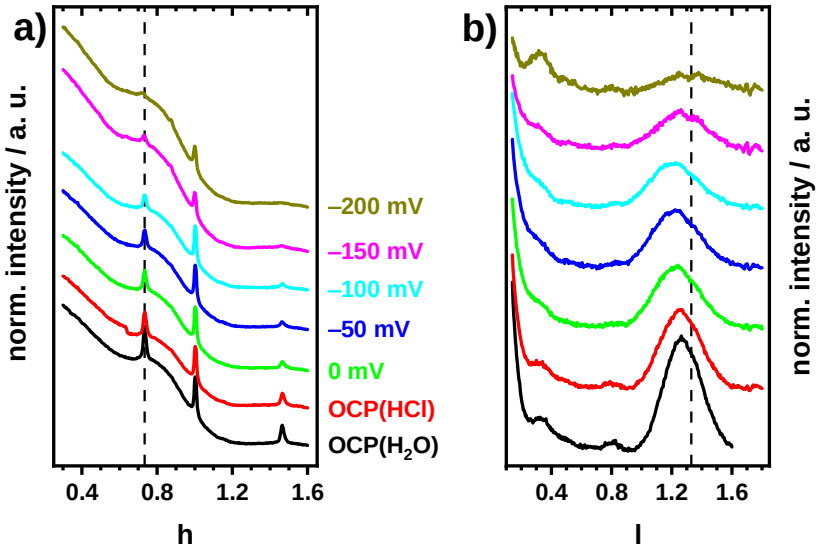

Figure 1: SXRD experiments of a nominal 1.66 nm thick RuO_2(110) layer grown on Ru(0001) in the HER potential region at various electrode potentials starting from OCP(H_2O), OCP(HCl) down to -200mV. a) h-scan at (k, l) = (0, 1.33) and b) l-scan at (h, k) = (0.73, 0). The strong background in the h-scans arises from diffuse scattering of the electrolyte. The dashed lines at h = 0.733 and l = 1.33 in the h- and l-scan, respectively, indicate the expected peak positions of RuO_2(110). The color code is valid for both h- and l-scans. The potential dependent scans are offset for clarity. A summary of all recorded h- and l-scans down to a potential of -1900 mV is shown in the **Figures S1** and **S2**, respectively.

In the corresponding l-scan at h = 0.73, k = 0 and OCP(HCl), a relatively broad maximum at l = 1.25 occurs that corresponds to a layer spacing of 3.4 Å, significantly larger than the RuO_2(110) bulk layer spacing of 3.23 Å[36]. Obviously even under OCP conditions the layer spacing of RuO_2(110) expands, presumably via proton incorporation, while the in-plane lattice vector of RuO_2(110) is not affected. From its full width of half maximum (FWHM) the

thickness of the RuO_2(110) layer is estimated to be 1.56 nm. In a control experiment the l-scans for OCP(HCl) with that of OCP(H_2O) for pure water are compared. The maximum in the l-scan was in the latter case at l = 1.27, indicating that the insertion of protons causes at least part of the observed expansion in the layer spacing of RuO_2(110).

With increasing cathodic potential the h-scans in **Figure 1a** change only little up to -100 mV, neither the intensity nor in the h-position of the RuO_2-related peaks change. At -150 mV both intensities of h = 0.73, 1.46 and h = 1 diminish by 50%. For an electrode potential of -200 mV the diffraction peak at h = 0.73 disappears almost completely in the h-scan, while the crystal truncation rod of Ru(0001) at h = 1.0 has not changed in intensity with respect to -150mV. From this experiment we conclude that the lateral periodicity of the RuO_2(110) layer has largely been destroyed under strong HER conditions (-200 mV *vs.* SHE), while the interface between the Ru(0001) and the reduced RuO_2(110) layer is still smooth.

A similar behavior is evident from the l-scans in **Figure 1b**. The integral intensity of the peak around l = 1.2-1.35 decreases continuously with increasing cathodic polarization, indicating a degradation in periodicity perpendicular to the RuO_2 film. At -100 mV the peak shifts to l = 1.22, that corresponds to an layer spacing in RuO_2(110) of 3.5 Å. The intensity of the peak decreases to 30%, while the FWHM varies only slightly. At an electrode potential of -150 mV, the peak shifts back to l = 1.27, i.e. RuO_2(110) layer spacing is 3.4 Å, while the intensity further decreases. At -200 mV only a weak feature at l = 1.32 remains that corresponds to a layer spacing of 3.2 Å, the nominal layer spacing of bulk RuO_2(110). Obviously, the perpendicular ordering of the Ru-O-Ru trilayers in the RuO_2(110) layer is almost lost at -200 mV.

The characteristic features (peak position, FWHM and intensity) derived from l-scans (SXRD) are summarized in **Figure 2**. In addition, there is a peak at l = 0.3 in the l-scans that is assigned to minor maximum of l = 0 peak due to the well-defined layer thickness of about 16 Å for the RuO_2 and reduced RuO_2 layer. The FWHM of the peak increases slightly as can be seen in the top of **Figure 2**. At OCP(H_2O) the FWHM is 0.30, which is associated with a layer thickness of 1.56 nm (4.9 layers)[35]. After polarization to -150 mV the FWHM slightly increased to 0.38, i.e., the thickness of the RuO_2(110) film decreased to 1.23 nm (3.8 layers). Due to low signal to noise ratio of the l = 1.3 peak below a polarization of -200 mV a reliable determination of the FWHM is not possible.

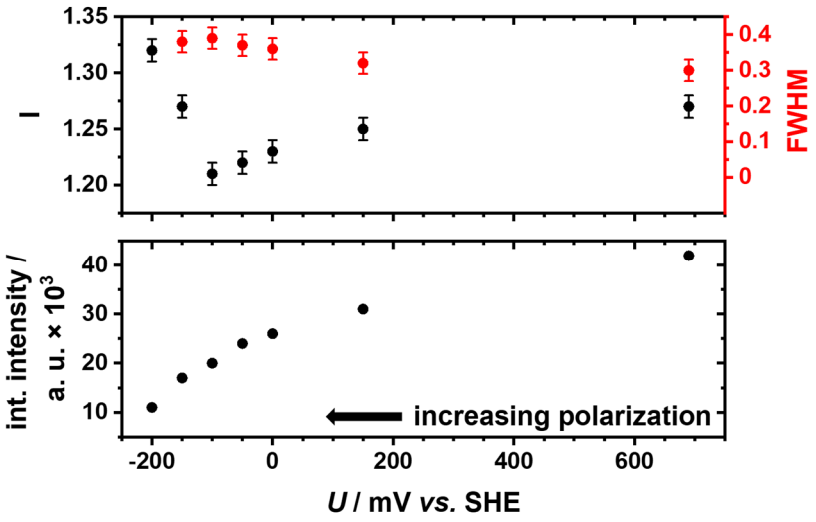

Figure 2: Peak position, FWHM (top) and integral intensity (bottom) derived from the l-scan data at (h, k) = (0.73, 0).

The FWHM of the peak at h = 0.73 at OCP(H_2O) is 0.018, which corresponds to a lateral dimension of 150 Å along the [-110] direction[35]. The FWHM, peak position, and the integral intensity derived from the h-scans are summarized in **Figure 3**. Both quantities remain constant upon potential variation. However, the integral intensity decreases continuously with increasing cathodic polarization (similar to the peak at l = 1.3 in the l-scan), indicating a continuous loss of lateral ordering of the film.

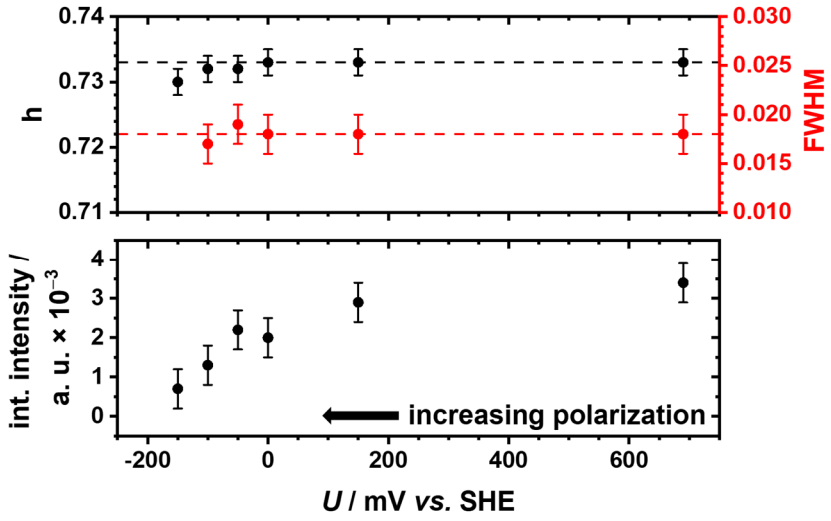

Figure 3: Peak position, FWHM (top) and integral intensity (bottom) derived from the h-scan data at (k, l) = (0, 1.33).

In conclusion, the SXRD experiments in **Figure 1** prove that polarization at -200 mV destroys the 3-dimensionally periodic structure of the 1.56 nm thick RuO_2(110) layer coated on Ru(0001). This "reduction" process of RuO_2(110) is irreversible, as RuO_2-related features do not recover after going back to lower cathodic potentials. In addition, from the h-scans it can be derived that the "reduction" process of the RuO_2(110) layer takes place domain-wise, since the peak positions and the FWHM values do not change during cathodic treatment, whereas the integral intensity decreases. Such a behavior of the RuO_2(110) surface under reducing conditions is known from previous UHV studies.[35,37]

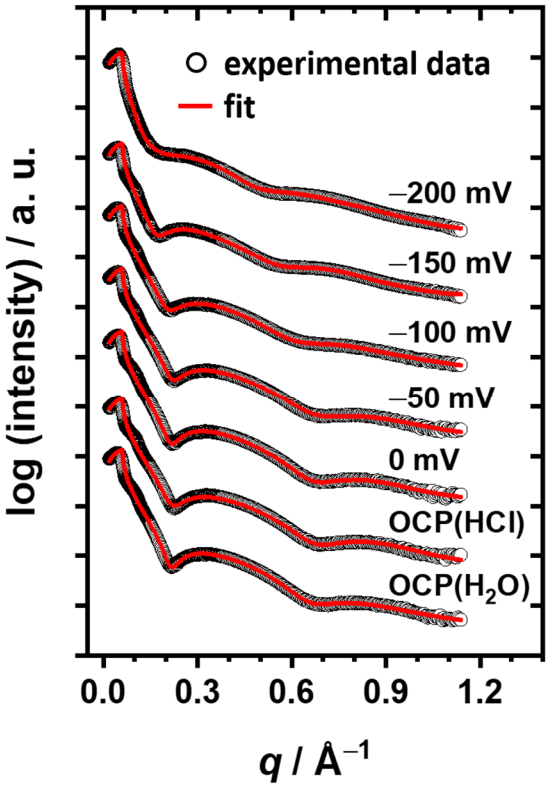

Figure 4: XRR experiments of a nominal 1.66 ± 0.04 nm thick RuO_2(110) layer supported on Ru(0001) in the HER potential region at various electrode potentials starting from OCP(H_2O), OCP(HCl) down to -200 mV. The potential dependent data sets are offset for clarity. A summary of all recorded XRR-scans down to a potential of -1900 mV is shown in **Figure S3**.

In **Figure 4** we present the XRR data as a function of the electrode potential. The black hollow circles represent the experimental data while the red solid lines show the simulation of the XRR data. For the simulations of the XRR data the software package GenX[38] (v 2.4.10) was used, employing a two-layer model for the measurements at OCP and the low cathodic potentials. For more cathodic potentials (-150 mV, -200 mV) a three-layer model was applied, both models

are depicted in the inset of **Figure 5**. The two-layer model consists of a layer with varying thickness and electron density (modelling the initial RuO_2(110) layer and the electrochemically reduced RuO_2 layer upon increasing polarization) that is followed by an interlayer with varying thickness and electron density (modelling the transition from the (reduced) oxide layer to the substrate) on the Ru(0001) substrate (cf. inset of **Figure 5**, all fitted data are summarized in **Table S1**). The simulation of the XRR data at more cathodic potentials required in addition a third layer denoted as "altered substrate". The most important parameters in the fitting the experimental XRR data are the thickness and the electron density of the (reduced) RuO_2 layer. For OCP, the XRR scan shows clear wiggles and minima from which the layer thickness can be determined quite accurately. The XRR scans for OCP(HCl) and OCP(H_2O) are virtually identical. In the present case an XRR analysis reveals a total thickness (RuO_2(110) layer plus interlayer) of the ultrathin film of 1.66 ± 0.04 nm. This value matches quite well the thickness estimation based on the SXRD data (1.56 nm). Since XRR is a dedicated method to determine layer thicknesses we use in the following 1.66 nm as the total thickness of our RuO_2(110)-based layer. With increasing cathodic electrode potential up to -200 mV, the RuO_2(110) layer change continuously in that the distinct minima shift to lower values for the scattering vector q in the XRR scans. This observation is indicative of the continuous increase in the layer thickness, i.e., the RuO_2(110) bulk layer swells, thereby increasing the total thickness from 1.66 ± 0.04 nm to 2.50 ± 0.04 nm (cf. **Figure 5**), while the O-Ru-O layer spacing increases first and then decreases (see l-scan in **Figure 1b**).

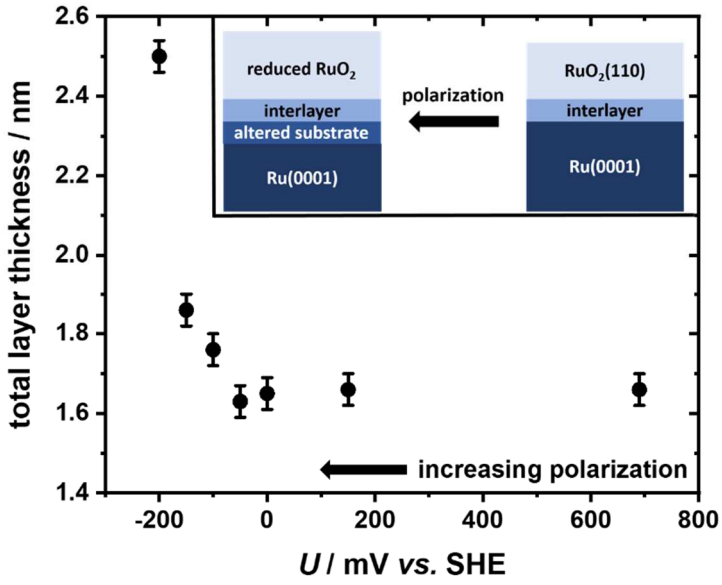

Figure 5: Total layer thickness ((reduced) RuO_2(110) layer plus interlayer) as derived from the fitting of the XRR data as a function of the electrode potential employing a two-layer

model (cf. inset, right) in the beginning and a three-layer model (cf. inset, left) at more cathodic potentials.

Most surprisingly, even at -200 mV a layer with well-defined thickness (i.e. distinct wiggles are discernible) is apparent in the XRR scan, although from SXRD the three-dimensional periodicity has practically been lost. The electron density of the reduced RuO_2 film reduces with the cathodic potential in a way that is consistent with the observed swelling of the layer due to proton insertion.

To complement these *in-situ* experiments, an identically prepared RuO_2(110) film was polarized in the HER potential region as described above and subsequently studied *ex-situ* by XPS and SEM. A comparison of the XP spectra of the freshly prepared RuO_2(110)/Ru(0001) electrode and after cathodic polarization is shown in **Figure S4**. O 1s and Ru 3d spectra after cathodic polarization are depicted and analyzed in **Figure 6**.

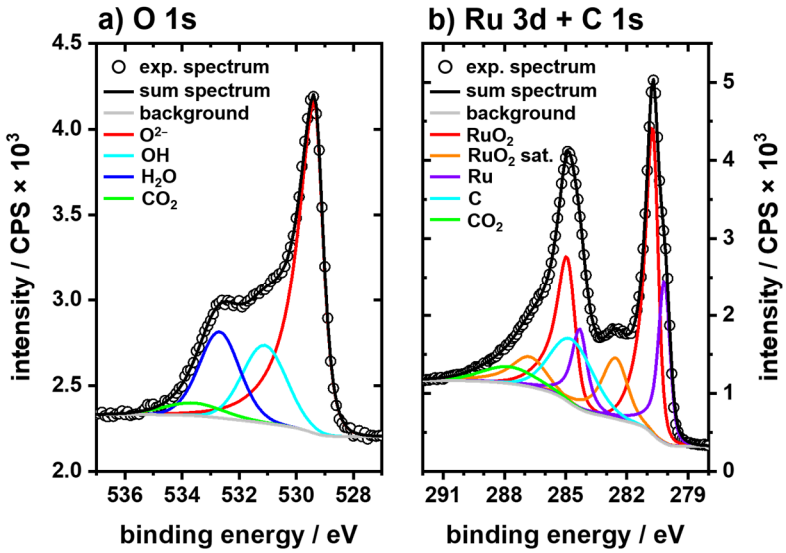

Figure 6: XP spectra of the RuO_2(110)/Ru(0001) electrode after the polarization of -200 mV where the crystallinity of the RuO_2(110) thin film almost disappeared. A peak fitting of the O 1s (a) and Ru 3d + C 1s (b) spectra was done according to literature.[42,43,44]

In the O 1s spectrum (**Figure 6a)**) up to four features are discernible. The one at a binding energy (BE) of 529.4 eV is assigned to bulk O in RuO_2[39,40], the two other emissions at 531.1 eV and 532.7 eV are ascribed to OH and H_2O in hydrous RuO_2, respectively[41,42], while the emission at 533.6 eV is assigned to dissolved CO_2[42]. CO_2 contamination has likely occurred during the transfer of the sample from the EC cell to the XPS apparatus through ambient atmosphere. The Ru 3d spectrum (**Figure 6b)**) consist of two (maybe composite) features at the energetic

positions of Ru $3d_{3/2}$ and Ru $3d_{5/2}$. Since the intensity ratio of Ru $3d_{5/2}$:Ru $3d_{3/2}$ is not 3:2 as expected from the degeneracy of both Ru 3d electronic transitions, we surmise that the peak at 285-286 eV consists of two contributions, one is related to Ru $3d_{3/2}$ at 285eV and the other one due to C 1s at 285-288 eV. Peak fitting of the Ru 3d and O 1s spectra are overlaid in **Figure 6**. The fitting parameters of the XP spectra are summarized in **Table S2**.

Quite similar XP spectra of O 1s and Ru 3d were reported for hydrous RuO_2 on single crystalline Ru(0001) that was prepared by anodic oxidation of Ru(0001).[42] Therefore, we conclude from SXRD, XRR and XPS experiments that the cathodic reduction of RuO_2(110) on Ru(0001) at -200 mV leads to the formation of a hydrous RuO_2 layer with a relatively sharp interface towards Ru(0001) and well-defined thickness.

With SEM we compare the RuO_2(110)/Ru(0001) before and after cathodic treatment in the HER potential region (cf. **Figure 7**). Obviously, there are changes in the morphology discernible. The freshly prepared RuO_2(110)/Ru(0001) surface (a) is flat with grain boundaries apparently visible (**Figure 7a**, dark contour lines). After cathodic treatment down to -200 mV the surface shows deposits in the form of rod-shape deposits (cf. **Figure 7b**) on the surface. These surface features are aligned along three high symmetry directions of the Ru(0001) substrate which in turn define the growth direction of RuO_2(110).

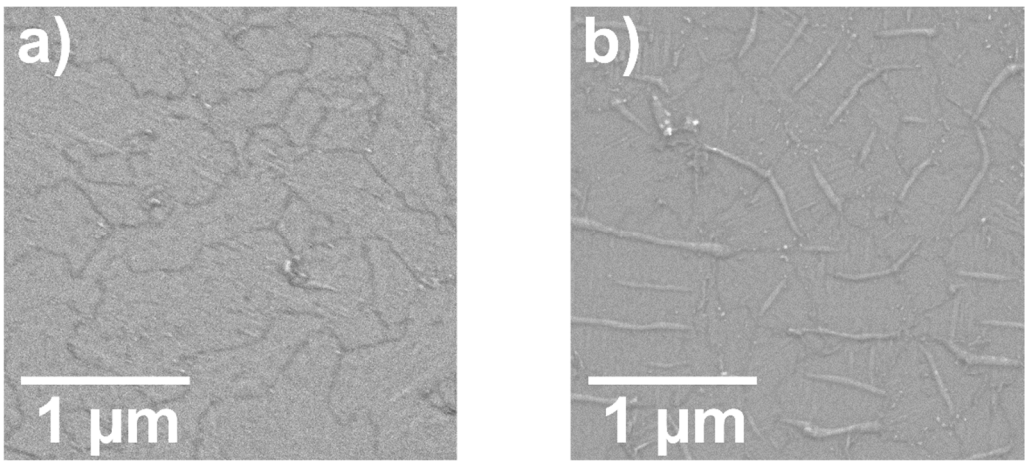

Figure 7: SE micrographs of a) freshly prepared RuO_2(110)/Ru(0001) and b) after polarization down to -200 mV in aqueous HCl solution (pH = 0.3).

While the previous characterization reveals changes in the crystal structure, morphology and chemical speciation of the RuO_2(110) ultrathin film during cathodic polarization in the HER potential region, cyclic voltammetry is able to emphasize alterations in the electrochemical

behavior. The cyclic voltammograms (CVs) recorded after the applying pulse-rest protocol (for details see the experimental part) with varying pulse potentials are depicted in **Figure 8**.

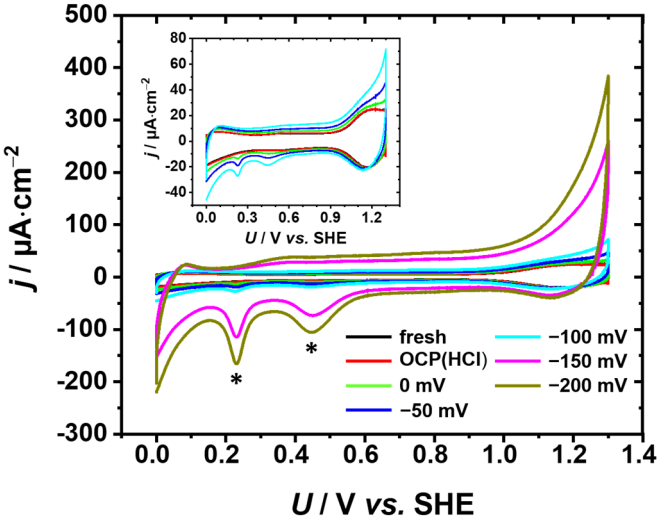

Figure 8: Cyclic voltammograms of the RuO_2(110) surface recorded during the cathodic treatment in aqueous 0.5 M HCl with a scan rate of 100 mV·s^{-1}. The legend gives the stationary pulse potentials which were applied for 30 s each. Evolving cathodic features of metallic Ru(0001) are marked with asterisks. The inset shows CVs with magnified current axis recorded right after immersion, the rest at OCP(HCl), and for various cathodic polarizations.

The freshly prepared RuO_2(110) surface was directly immersed in 0.5 M HCl. The CV of the clean surface is shown as black line in **Figure 8** and is in good agreement with a covering RuO_2(110) layer.[29] An enlarged depiction of the inset is shown in **Figure S5**. After resting at OCP(HCl) (red line) for 55 min the CV is almost identical to the one right after immersing the electrode (cf. **Figure S5**). When the first pulse-rest procedure was conducted at a potential of 0 mV, additional small cathodic features appear in the CV around 0.23 V and 0.45 V (marked with an asterisk) that become more pronounced when going to more cathodic potentials of -150 mV and -200 mV. These cathodic features in CV are ascribed to the metallic Ru(0001) surface.[45-48] Furthermore the capacitive current density increases slightly from OCP(HCl) to -100 mV and then (abruptly) doubles approximately above -150 mV. This rise in the capacitive current density may indicate an increase in the electrochemically active surface area that is caused by the pseudocapacity of hydrous RuO_2. At the same time the OER activity (current above 1.23 V) increase significantly by a factor of four. Both findings may be attributed to the formation of hydrous RuO_2 and metallic Ru[49] with their higher activity in OER than stoichiometric RuO_2.

4. Discussion

From SXRD, XRR, XPS, and CV experiments it is concluded that a 1.66 nm thick single-crystalline RuO_2(110) layer transforms into hydrous RuO_2 and metallic Ru for cathodic electrode potentials below -150 mV. Similar conclusions were previously drawn for polycrystalline RuO_2 electrodes.[12,17] From the Pourbaix diagram of ruthenium we would have expected that RuO_2 fully transforms to metallic ruthenium under such reducing conditions.[20] However, this is only observed in the CV of the model electrode treated at -200 mV, but XPS indicates clearly the presence of hydrous RuO_2. Obviously, not thermodynamics but also kinetics determines the (meta)stability of (hydrous) RuO_2 under acidic HER conditions.

At low cathodic electrode potentials the layer spacing of RuO_2(110) increased (cf. **Figure 2**, SXRD) due presumably to proton incorporation into the RuO_2 lattice. This increase in layer distance of RuO_2(110) upon contact to aqueous HCl solution at low cathodic potentials agrees remarkably well with previous studies on RuO_2 thin films.[28] At more cathodic potential (-150 mV to -200 mV) the RuO_2(110) layer transforms into a material with no long range order. Presumably hydrous RuO_2 is formed when considering the XPS data in comparison with a recent study of model hydrous RuO_2 on Ru(0001) prepared under OER conditions.[42] Since hydrous RuO_2 contains OH and water, as identified by *ex-situ* XPS (cf. **Figure 6**), the strongly reduced RuO_2 layer (polarized to cathodic potential -150 mV) swelled as evidenced by an increase of the layer thickness from 1.66 ± 0.04 nm to 2.50 ± 0.04 nm as observed in XRR (cf. **Figure 5**). The supposed massive insertion of protons into the RuO_2 lattice below -150 mV keeps the octahedral coordination of Ru, but destroys the connectivity among the Ru-octahedrons and thus the crystallinity of reduced RuO_2 layer (SXRD, cf. **Figures 1, 2, 3**) accompanied by a swelling of the layer (XRR) by around 0.8 nm (cf. **Figure 5**).

The formation of hydrous RuO_2 film is reconciled with a significantly higher capacitive current densities in cyclic voltammetry after cathodic polarization below -150 mV (cf. **Figure 8**) and also by the higher current density in the OER region. CVs before and after cathodic polarization support this view and additionally indicate that metallic ruthenium is exposed to the electrolyte. The cathodic features of Ru(0001) start to evolve after polarization to 0 mV already, but the general shape of the RuO_2(110) cyclic voltammogram is largely preserved at least up to a potential pulse of -100 mV. After cathodic polarization to -150 mV the Ru(0001) related features are much more pronounced.

The reduction of RuO_2(110) under cathodic polarization in the HER potential region can also be compared with the chemical reduction of RuO_2(110) by exposing the surface to gaseous H_2. Even at room temperature reduction with gaseous H_2 is able to form water at RuO_2(110) surface[50], but this treatment is not able to further reduce the bulk of RuO_2(110). Only at 450 K H_2 exposure reduces the bulk of the RuO_2(110) layer slowly to metallic Ru (10^{-5} mbar within 1h).[35] Since the HER at RuO_2(110) proceeds at room temperature, full reduction to metallic Ru may be suppressed. Altogether, we anticipate that the evolved H_2 at the cathode will not be able to reduce the RuO_2(110) layer. Instead, the electrochemical reduction involves a sequence of consecutive coupled protonation and electron transfer step.

In the following we provide an educated guess for the mechanism of the electrochemical reduction of a RuO_2(110) layer in acidic environment that is based on the presented experimental results. For cathodic potentials protons penetrate the RuO_2(110) layer and are inserted by a coupled proton plus electron transfer and it comes to a reduction of Ru from oxidation state from IV to III and to finally 0 for metallic ruthenium. For low potentials down to -100 mV *vs.* SHE proton insertion results in the transformation of lattice O into hydroxyl groups and the reduction of Ru^{IV} to Ru^{III}. Both steps cause an expansion of the interlayer spacing of RuO_2(110) as evidenced by SXRD without changing the local octahedral coordination of Ru. Since the crystallinity of the RuO_2(110) film is still high (SXRD), the connectivity of most of the Ru-O_6 octahedrons is assumed to be still intact. However, the formation of hydroxyl groups will lead to rehybridization of O from sp^2 to sp^3 thereby weakening the O-Ru bonding (conservation of bond order). Below a cathodic potential of -150 mV *vs.* SHE and therefore with increasing degree of protonation this bond weakening will lead to O-Ru bond breaking and a loss of the connectivity of the Ru-O_6 octahedrons. In the SXRD experiments the O-Ru bond breaking is reflected by a diminishing crystallinity of the electrochemically reduced RuO_2(110) film. As long as the covering film does not dissolve, a well-defined layer is maintained as evidenced by XRR experiments whose layer thickness has increased (XRR). This part of the mechanism of the electrochemical reduction of the RuO_2(110) layer can be considered as “homogeneous” transformation.

In summary, we suggest the “homogeneous” electrochemical reduction to proceed via the following steps:

(1) $Ru^{IV}O_2 + H^+ + e^- \rightleftharpoons Ru^{III}O(OH)$

(2) $Ru^{III}O(OH) + H^+ + e^- \rightleftharpoons Ru^{II}(OH)_2$

(3) $Ru^{II}(OH)_2 + H^+ + e^- \rightleftharpoons Ru^{I}(OH) + H_2O$

(4) $Ru^{I}(OH) + H^{+} + e^{-} \rightleftharpoons Ru^{0} + H_2O$

However, the connectivity of the Ru octahedral can even be reduced to a degree that soluble Ru-complexes are formed with enhanced mobility in the electrochemical double layer. The chemical nature of such complexes are not precisely known, however, they are likely to be Ru-oxyhydroxide complexes. We can presume neutral Ru complexes to be solvated; negative Ru complexes are unlikely, while positive Ru complexes will not leave the cathode. After additional protonation of the solvated neutral Ru complex the cation is re-deposited on the surface. This solvation and protonation process provides the required mobility for the "heterogeneous" transformation that is evidenced from SEM experiments. We recognize deposition in the form of rod-shaped structures on the surface that are likely formed by nucleation and growth (heterogeneous growth).

Just for comparison reasons we address briefly the electrochemical reduction of RuO_2 in alkaline conditions, a process that may be substantially different. While protons H^+ can easily penetrate the bulk of a RuO_2 film, this is not be the case for water that is split to hydroxyls OH^- and adsorbed hydrogen atoms under alkaline conditions. Water can only interact at the surface of RuO_2(110) and adsorbed H is immobile at room temperature.[40,51] Therefore, we anticipate that bulk RuO_2 (110) under alkaline conditions is more reluctant to electrochemical reduction and will form smoother reduced RuO_2 films than under acidic conditions.

The observed reduction process of a 1.66 nm thick RuO_2(110) layer is not in contradiction with a previous study by Lister et al.[30]. In their study a bulk RuO_2 single crystal was employed as model cathode and *in-situ* SXRD did not indicate any alterations in the crystallinity of RuO_2 except that the roughness of the surface increased. However, even if bulk RuO_2 is partly reduced at the surface, the hydrous RuO_2 part is likely to be not crystalline and therefore invisible in SXRD, while the remaining RuO_2 core is still fully visible in XRD.

Quite in contrast, in our study a 1.66 nm thick RuO_2(110) layer on Ru(0001) was employed and as soon as this single crystalline film loses part of its crystallinity the RuO_2-related X-ray diffraction peaks are strongly affected. This is also the appeal of our present approach using well-designed model electrodes. The reduction of a ultrathin RuO_2(110) layer on Ru(0001) is a well-designed experiment in that the cathodic polarization in the HER potential region attacks only the RuO_2(110) layer but leaves the underlying Ru(0001) substrate fully intact. Therefore, after electrochemical reduction the RuO_2-based layer exhibits a sharp hydrous RuO_2/Ru(0001) interface as reconciled with XRR and quite in contrast to the recently reported preparation of hydrous RuO_2 by anodic oxidation of Ru(0001).[42] From a preparation point of view the

reduction of RuO_2(110) in the potential region of HER opens the way to produce a hydrous RuO_2 layer with a well-controlled thickness that can be used as a model catalyst for studying for instance the catalytic dehydrogenation reactions in detail.

Conclusions

We prepared a ultrathin (1.66 ± 0.04 nm thick) single crystalline RuO_2(110) film fully covering the Ru(0001) substrate that served as a model cathode for the electrochemical reduction of RuO_2(110) in the potential region of HER in acidic environment and was studied by *in-situ* SXRD and XRR experiments and supplemented by *ex-situ* XPS, CV, and SEM experiments. With this experiment we demonstrate that in acidic medium RuO_2(110) can be electrochemically reduced (homogeneous transformation) to a hydrous RuO_2 layer with well-defined thickness and rod-shape deposits (heterogeneous transformation). We propose that for cathodic potentials protons penetrate the RuO_2(110) layer and are inserted by a coupled proton and electron transfer, thereby transforming lattice O to OH and water and reducing the oxidation state of Ru. Upon cathodic polarization in the HER potential region (down to -100 mV *vs.* SHE), first a variation of the layer spacings of RuO_2(110) was observed with SXRD that is ascribed to proton insertion into the RuO_2 lattice, maintaining the octahedral coordination of Ru and proper connectivity of the octahedrons (rutile structure). Proceeding to even further cathodic potentials destroys the crystallinity of the RuO_2(110) layer (h- and l-scans in SXRD), presumably by transforming lattice O into OH and H_2O, thereby breaking the connectivity among the Ru-octahedrons. For a cathodic potential of -200 mV the periodicity of the RuO_2(110) is lost. The formation of OH and water into the RuO_2 lattice leads to swelling of the layer (observed in XRR). Spectroscopic signatures in O 1s and Ru 3d XP spectra are compatible with the formation of hydrous RuO_2.

Supporting Information

- complete experimental SXRD and XRR data sets

- comparison of XP spectra before and after polarization

- fitting parameters for XPS and XRR data

- enlarged depiction of the inset of Figure 8

Acknowledgements

We thank financial support by the BMBF (project: 05K2016-HEXCHEM).

References:

(1) Crabtree, G. W.; Dresselhaus, M. S.; Buchanan, M. V. The Hydrogen Economy. *Phys. Today* **2004**, *57*, 39-45.

(2) Ursua, A.; Gandia, L. M.; Sanchis, P. Hydrogen Production from Water Electrolysis: Current Status and Future Trends. *Proc. IEEE* **2012**, *100*, 410-426.

(3) Barber, J.; Conway, B. E. Structural Specificity of the Kinetics of the Hydrogen Evolution Reaction on the Low-Index Surfaces of Pt Single-Crystal Electrodes in 0.5 M dm^{-3} NaOH. *J. Electroanal. Chem.* **1999**, *461*, 80-89.

(4) Markovic, N. M.; Ross, P. N. New Electrocatalysts for Fuel Cells: From Model Surfaces to Commercial Catalysts. *Cat. Tech.* **2000**, *4*, 110-126.

(5) Kibler, L. A. Hydrogen Electrocatalysis. *Chem. Phys. Chem.* **2006**, *7*, 985-991.

(6) Breiter, M. W. in: Vielstich, W.; Lamm, A.; Gasteiger, H. [Eds.] *Handbook of Fuel Cells: Fundamentals, Technology and Applications, Vol. 2*; Wiley: Chichester, U.K., 2003.

(7) Zheng, Y.; Jiao, Y.; Jaroniec, M.; Qiao, S. Z. Advancing the Electrochemistry of the Hydrogen-Evolution through Combining Experiment and Theory. *Angew. Chem. Int. Ed.* **2015**, *54*, 52-65.

(8) Beard, B. C.; Ross, P. N. The Structure and Activity of Pt-Co Alloys as Oxygen Reduction Electrocatalysts. *J. Electrochem. Soc.* **1990**, *137*, 3368-3374.

(9) Stamenkovic, V. R.; Fowler, B.; Mun, R. S.; Wang, G.; Ross, P. N.; Lucas, C. A.; Markovic, N. M. Improved Oxygen Reduction Activity on $Pt_3Ni(111)$ via Increased Surface Site Availability. *Science* **2007**, *315*, 493-497.

(10) Galizzioli, D.; Tantardini, F.; Trasatti, S. Ruthenium Dioxide: A New Electrode Material. I. Behaviour in Acid Solutions of Inert Electrolytes. *J. Appl. Electrochem.* **1974**, *4*, 57-67.

(11) Nidola, A.; Schira, R. Poisoning Mechanisms and Structural Analyses on Metallic Contaminated Cathode Catalysts in Chlor-Alkali Membrane Cell Technology. *J. Electrochem. Soc.* **1986**, *133*, 1653-1656.

(12) Kötz, E. R.; Stucki, S. Ruthenium Dioxide as a Hydrogen-Evolving Cathode. *J. Appl. Electrochem.* **1987**, *17*, 1190-1197.

(13) Ardizzone, S.; Fregonara, G.; Trasatti, S. Influence of Hydrogen Evolution on the Voltammetric Charge of RuO_2 Electrodes. *J. Electroanal. Chem.* **1989**, *266*, 191-195.

(14) Boodts, J. C. F.; Trasatti, S. Hydrogen Evolution on Iridium Oxide Cathodes. *J. Appl. Electrochem.* **1989**, *19*, 255-262.

(15) Wen, T.-C.; Hu, C.-C. Hydrogen and Oxygen Evolutions on Ru-Ir Binary Oxides. *J. Electrochem. Soc.* **1992**, *139*, 2158-2163.

(16) Cornell, A.; Simonsson, D. Ruthenium Dioxide as Cathode Material for Hydrogen Evolution in Hydroxide and Chlorate Solutions. *J. Electrochem. Soc.* **1993**, *140*, 3123-3129.

(17) Blouin, M.; Guay, D. Activation of Ruthenium Oxide, Iridium Oxide, and Mixed Ru_xIr_{1-x} Oxide Electrodes during Cathodic Polarization and Hydrogen Evolution. *J. Electrochem. Soc.* **1997**, *144*, 573-581.

(18) T. F. O'Brien, T. V. Bommaraju, F. Hine, *Handbook of Chlor-Alkali Technology*, Springer, New York, **2005**

(19) Holmin, S.; Näslund, L.-A.; Ingason, A. S.; Rosen, J.; Zimmerman, E. Corrosion of Ruthenium Dioxide Based Cathodes in Alkaline Medium Caused by Reverse Currents. *Electrochim. Acta* **2014**, *146*, 30-36.

(20) Pourbaix, M. *Atlas of Electrochemical Equilibria in Aqueous Solutions*; Pergamon Press: Oxford, U.K., 1966.

(21) Iwakura, C.; Tanaka, M.; Nakamatsu, S.; Inoue, H.; Matsuoka, M.; Furukawa, N. Electrochemical Properties of Ni/(Ni+RuO_2) Active Cathodes for Hydrogen Evolution in Chlor-Alkali Electrolysis. *Electrochim. Acta.* **1995**, *40*, 977-982.

(22) Hachiya, T.; Sasaki, T.; Tsuchida, K.; Houda, H. Ruthenium Oxide Cathodes for Chlor-Alkali Electrolysis. *ECS Trans.* **2009**, *16*, 31-49.

(23) Näslund, L.-A.; Ingason, A. S.; Holmin, S.; Rosen, J. Formation of $RuO(OH)_2$ on RuO_2-Based Electrodes for Hydrogen Production. *J. Phys. Chem. C* **2014**, *118*, 15315-15323.

(24) Karlsson, R. K. B.; Cornell, A.; Petterson, L. G. M. Structural Changes in RuO_2 during Electrochemical Hydrogen Evolution. *J. Phys. Chem. C* **2016**, *120*, 7094-7102.

(25) Chu, Y. S.; Lister, T. E.; Cullen, W. G.; You, H.; Nagy, Z. Commensurate Water Monolayer at the RuO_2(110)/Water Interface. *Phys. Rev. Lett.* **2001**, *86*, 3364-3367.

(26) Chabanier, C.; Irissou, E.; Guay, D.; Pelletier, J. F.; Sutton, M.; Lurio, L. B. Hydrogen Absorption in Thermally Prepared RuO_2 Electrode. *Electrochem. Solid-State Lett* **2002**, *5*, E40-E42.

(27) Rochefort, D.; Dabo, P.; Guay, D.; Sherwood, P. M. A. XPS Investigations of Thermally Prepared RuO_2 Electrodes in Reductive Conditions. *Electrochim. Acta* **2003**, *48*, 4245-4252.

(28) Chabanier, C.; Guay, D. Activation and Hydrogen Absorption in Thermally Prepared RuO_2 and IrO_2. *J. Electroanal. Chem.* **2004**, *570*, 13-27.

(29) Lister, T. E.; Chu, Y.; Cullen, W.; You, H.; Yonco, R. M.; Mitchell, J. F.; Nagy, Z. Electrochemical and X-ray Scattering Study of Well Defined RuO_2 Single Crystal Surfaces. *J. Electroanal. Chem.* **2002**, *524-525*, 201-218.

(30) Lister, T. E.; Tolmachev, Y. V.; Chu, Y.; Cullen, W. G.; You, H.; Yonco, R.; Nagy, Z. Cathodic Activation of RuO_2 Single Crystal Surfaces for Hydrogen-Evolution Reaction. *J. Electroanal. Chem.* **2003**, *554-555*, 71-76.

(31) Herd, B.; Knapp, M.; Over, H. Atomic Scale Insights into the Initial Oxidation of Ru(0001) Using Molecular Oxygen: A Scanning Tunneling Microscopy Study. *J. Phys. Chem C.* **2012**, 116, 24649-24660.

(32) Sohrabnejad-Eskan, I.; Goryachev, A.; Exner, K. S.; Kibler, L. A.; Hensen, E. J. M.; Hofmann, J. P.; Over, H. Temperature-Dependent Kinetic Studies of the Chlorine Evolution Reaction over RuO_2(110) Model Electrodes. *ACS Catal.* **2017**, *7*, 2403-2411.

(33) Foresti, M. L.; Pozzi, A.; Innocenti, M.; Pezzatini, G.; Loglio, F.; Salvietti, E.; Giusti, A.; D'Anca, F.; Felici, R.; Borgatti, F. In Situ Analysis Under Controlled Potential Conditions: An Innovative Setup and its Application to the Investigation of Ultrathin Films Electrodeposited on Ag(111). *Electrochim. Acta* **2006**, *51*, 5532-5539.

(34) Zhang, F.; Evertsson, J.; Bertram, F.; Rullik, L.; Carla, F.; Långberg, M.; Lundgren, E.; Pan, J. Integration of Electrochemical and Synchrotron-Based X-Ray Techniques for *In-Situ* Investigation of Aluminium Anodization. *Electrochim. Acta* **2017**, *241*, 299-308.

(35) He, Y. B.; Knapp, M.; Lundgren, E.; Over, H. Ru(0001) Model Catalyst under Oxidizing and Reducing Reaction Conditions: In-Situ High-Pressure Surface X-ray Diffraction Study. *J. Phys. Chem. B* **2005**, *109*, 21825-21830.

(36) Kim, Y. D.; Seitsonen, A. P.; Over, H. The Atomic Geometry of Oxygen-Rich Ru(0001) surfaces: Coexistence of (1×1)O and RuO_2(110) Domains. *Surf. Sci.* **2000**, *465*, 1-8.

(37) Kim, S. H.; Wintterlin, J. Morphology of RuO_2(110) Oxide Films on Ru(0001) Studied by Scanning Tunneling Microscopy. *J. Chem. Phys.* **2009**, *131*, 064705.

(38) Björck, M.; Andersson, G. *GenX*: An Extensible X-Ray Reflectivity Refinement Program Utilizing Differential Evolution. *J. Appl. Cryst.* **2007**, *40*, 1174-1178.

(39) Over, H.; Seitsonen, A. P.; Lundgren, E.; Wiklund, M.; Andersen, J. N. Spectroscopic Characterization of Catalytically Active Surface Sites of a Metal Oxide. *Chem. Phys. Lett.* **2001**, *342*, 467-472.

(40) Knapp, M.; Crihan, D.; Seitsonen, A. P.; Lundgren, E.; Resta, A.; Andersen, J. N.; Over, H. Complex Interaction of Hydrogen with the RuO_2(110) Surface. *J. Phys. Chem. C* **2007**, *111*, 5363-5373.

(41) Foelske, A.; Barbieri, O.; Hahn, M.; Kötz, R. An X-Ray Photoelectron Spectroscopy Study of Hydrous Ruthenium Oxide Powders with Various Water Contents for Supercapacitors. *Electrochem. Sol. Stat. Lett.* **2006**, *9*, A268-A272.

(42) Krause, P. P. T.; Camuka, H.; Leichtweiss, T.; Over, H. Temperature-Induced Transformation of Electrochemically Formed Hydrous RuO_2 layers over Ru(0001) Model Electrodes. *Nanoscale* **2016**, *8*, 13944-13953.

(43) Over, H. Surface Chemistry of Ruthenium Dioxide in Heterogeneous Catalysis and Electrocatalysis: From Fundamental to Applied Research. *Chem. Rev.* **2012**, 116, 3356-3426.

(44) Morgan, D. J. Resolving Ruthenium: XPS Studies of Common Ruthenium Materials. *Surf. Interface Anal.* **2015**, *47*, 1072-1079.

(45) Brankovic, S. R.; Wang, J. X.; Zhu, Y.; Sabatini, R.; McBreen, J.; Adžić, R. R. Electrosorption and Catalytic Properties of Bare and Pt Modified Single Crystal and Nanostructured Ru Surfaces. *J. Electroanal. Chem.* **2002**, *524-525*, 231-241.

(46) Marinković, N. S.; Wang, J. X.; Zajonz, H.; Adžić, R. R. Adsorption of Bisulfate on the Ru(0001) Single Crystal Electrode Surface. *J. Electroanal. Chem.* **2001**, *500*, 388-394.

(47) Vukmirovic, M. B.; Sabatini, R. L.; Adžić, R. R. Growth of RuO_2 by Electrochemical and Gas-Phase Oxidation of an Ru(0001) Surface. *Surf. Sci.* **2004**, *572*, 269-276.

(48) Wang, J. X.; Marinković, N. S.; Zajonz, H.; Ocko, B. M.; Adžić, R. R. In Situ X-Ray Reflectivity and Voltammetry Study of Ru(0001) Surface Oxidation in Electrolyte Solutions. *J. Phys. Chem. B* **2001**, *105*, 2809-2814.

(49) Cherevko, S.; Geiger, S.; Kasian, O.; Kulyk, N.; Grote, J.-P.; Savan, A.; Shrestha, B. R.; Merzlikin, S.; Breitbach, B.; Ludwig, A. *et al*. Oxygen and Hydrogen Evolution Reactions on Ru, RuO_2, Ir , and IrO_2 Thin Film Electrodes in Acidic and Alkaline Electrolytes: A Comparative Study on Activity and Stability. *Catal. Today* **2016**, *262*, 170-180.

(50) Knapp, M.; Crihan, D.; Seitsonen, A. P.; Resta, A.; Lundgren, E.; Andersen, J. N.; Schmid, M.; Varga, P.; Over, H. Unusual Process of Water Formation on RuO_2(110) by Hydrogen Exposure at Room Temperature. *J. Phys. Chem. Lett.* **2006**, *110*, 14007-14010.

(51) Dahal, A.; Mu, R.; Lyubinetsky, I.; Dohnálek, Z. Hydrogen Adsorption and Reaction on RuO_2(110). *Surf. Sci.* **2018**, *677*, 264-270 and references therein.

TOC Graphics